Mol Genet Genomics (2013) 288:413–424
DOI 10.1007/s00438-013-0756-6

ORIGINAL PAPER

Random mutagenesis identifies factors involved in formate-dependent growth of the methanogenic archaeon *Methanococcus maripaludis*

Christian Sattler · Sandro Wolf · Julia Fersch · Stefan Goetz · Michael Rother

Received: 19 December 2012 / Accepted: 31 May 2013 / Published online: 26 June 2013

Abstract Methane is a key intermediate in the carbon cycle and biologically produced by methanogenic archaea. Most methanogens are able to conserve energy by reducing CO_2 to methane using molecular hydrogen as electron donor (hydrogenotrophic methanogenesis), but several hydrogenotrophic methanogens can also use formate as electron donor for methanogenesis. Formate dehydrogenase (Fdh) oxidizes formate to CO_2 and is involved in funneling reducing equivalents into the methanogenic pathway, but details on other factors relevant for formate-dependent physiology of methanogens are not available. To learn more about the factors involved in formate-dependent growth of *Methanococcus maripaludis* strain JJ, we used a recently developed system for random in vitro mutagenesis, which is based on a modified insect transposable element to create 2,865 chromosomal transposon mutants and screened them for impaired growth on formate. Of 12 *M. maripaludis* transposon-induced mutants exhibiting this phenotype, the transposon insertion sites in the chromosome were mapped. Among the genes, apparently affecting formate-dependent growth were those encoding archaeal transcription factor S, a regulator of ion transport, and carbon monoxide dehydrogenase/acetyl-CoA synthase. Interestingly, in seven of the mutants, transposons were localized in a 10.2 kb region where Fdh1, one of two Fdh isoforms in the organism, is encoded. Two transcription start sites within the 10.2 kb region could be mapped, and quantification of transcripts revealed that transposon insertion in this region diminished *fdhA1* expression due to polar effects.

Keywords *Methanococcus maripaludis* · Transposon · Himar1 · Mutagenesis · Formate · Methanogenesis · Selenocysteine

Nucleotide sequence data reported are available in the GenBank database under accession number KC342234.

Communicated by G. Klug.

Electronic supplementary material The online version of this article (doi:10.1007/s00438-013-0756-6) contains supplementary material, which is available to authorized users.

C. Sattler · S. Wolf · J. Fersch · M. Rother (✉)
Institut für Mikrobiologie, Technische Universität Dresden, 01062 Dresden, Germany
e-mail: michael.rother@tu-dresden.de

C. Sattler · S. Goetz · M. Rother
Institut für Molekulare Biowissenschaften, Johann Wolfgang Goethe-Universität Frankfurt, Frankfurt, Germany

Introduction

Biological methane production, methanogenesis, is carried out exclusively by methanogenic members of the Euryarchaeota, one of the major kingdoms of the Archaea. In the absence of external electron acceptors, such as oxygen, nitrate, sulfate, or metals, these organisms play a key role in the anaerobic degradation of biomass. Most methanogenic archaea are able to thrive by reduction of CO_2 to methane using molecular hydrogen as electron donor. In this pathway, hydrogenotrophic methanogenesis, CO_2 is reduced to methane in seven steps involving coenzyme-bound C1 intermediates (Thauer 1998). During this process, a proton and/or sodium ion motive force across the cytoplasmic membrane is generated which drives ATP synthesis by ATP synthase and other energy-requiring reactions (Deppenmeier and Müller 2008). Beside $H_2 + CO_2$, formate can also serve as the energy source for

several hydrogenotrophic methanogens, but in-depth knowledge about their formate-dependent physiology is rather scarce. Formate dehydrogenase (Fdh) oxidizes formate to CO_2 using cofactor F_{420} (a deazaflavin derivative functionally analogous to NAD^+) as electron acceptor (Ferry 1990). Reduced F_{420} or H_2 can serve as electron donor for CO_2 reduction to methane (Lie et al. 2012). In some hydrogenotrophic methanogens, such as *Methanococcus maripaludis*, Fdh contains the unusual amino acid selenocysteine (sec), which is co-translationally inserted and encoded by the stop codon UGA on the mRNA (Stock and Rother 2009). Therefore, formate-dependent growth of *M. maripaludis* requires selenium and an intact pathway for sec biosynthesis and incorporation (Stock et al. 2010). *M. maripaludis* strain S2, for which the genome sequence is available (Hendrickson et al. 2004) synthesizes two sec-containing Fdhs, Fdh1 (encoded by sec-encoding *fdhA1* and *fdhB1*), and Fdh2 (encoded by sec-encoding *fdhA2* and *fdhB2*) and either one alone is sufficient to enable the organism to grow on formate. In the absence of Fdh1, prolonged incubation is required presumably because *fdh2* is expressed at a higher level only under hydrogen-limiting conditions (Costa et al. 2013; Lupa et al. 2008; Wood et al. 2003). *M. maripaludis* strain JJ, for which no genome sequence is available also encodes two sec-containing Fdhs, but *fdh2* is barely expressed under laboratory conditions (Stock et al. 2011). Conversely, *fdhA1* of *M. maripaludis* JJ is expressed at a high level regardless if the organism grows on $H_2 + CO_2$ or formate. This situation is thought to ensure the preferred insertion of sec during translation into Fdh over the other sec-containing proteins, which are regulated in response to the selenium status and for which sec-independent isoforms are synthesized upon selenium deprivation or disruption of the pathway for sec biosynthesis and incorporation (Stock et al. 2011).

M. maripaludis is one of the few model methanogens with an established system for facile genetic manipulation. This includes efficient transformation and plating procedures, availability of marker genes for screening and selection purposes, and shuttle vectors (Leigh et al. 2011; Sarmiento et al. 2011). We recently reported on a system for random in vitro mutagenesis of *M. maripaludis* (Rother et al. 2011) employing a tailored insect transposable element of the *mariner* family, *Himar1*, originally developed for in vivo mutagenesis of *Methanosarcina acetivorans* (Zhang et al. 2000). The modified mini-*Himar1* element used (mini-MAR367) carries a puromycin resistance cassette (for selection in *Methanococcus*) as well as an *Escherichia coli* selectable marker and plasmid origin of replication allowing facile cloning of transposon insertions to identify the mutated gene. Here, we applied this system to isolate randomly generated *M. maripaludis* mutants in which formate-dependent—but not $H_2 + CO_2$-dependent—growth was affected. This procedure led to the characterization of different *fdh*-encoding transcripts and to the identification of previously unrecognized factors involved in formate-dependent catabolism, thus exemplifying the use of random genetic analysis of *M. maripaludis*.

Materials and methods

Strains, media, and growth conditions

E. coli strains were grown under standard conditions (Wanner 1986) and transformed with plasmid DNA by electroporation (Fiedler and Wirth 1988). For selection of plasmids, ampicillin (100 μg/ml) or kanamycin (50 μg/ml) was added to the media. *M. maripaludis* JJ (DSMZ 2067; Jones et al. 1983) and its derivatives (Table 1) were cultivated at 37 °C in McSe medium (Rother et al. 2003) containing casamino acids (Whitman et al. 1986), 10 mM (or 50 mM where indicated) sodium acetate, and 1 μM sodium selenite. Either 2×10^5 Pa H_2:CO_2 (80:20) or 2 % (w/v) sodium formate served as the sole energy source. For the latter condition, 80 mM morpholinepropanesulfonic acid, pH 6.8, was added to keep the pH constant, and the headspace contained 0.5×10^5 Pa of N_2:CO_2 (80:20). *M. maripaludis* was shifted from hydrogenotrophic to formate-dependent growth conditions using a 4 % inoculum of an overnight culture. Transformation of *M. maripaludis*, plating on solid media, and selection for resistance toward puromycin were conducted as described previously (Tumbula et al. 1994; Stock et al. 2010). The inability of transposon-induced *M. maripaludis* mutants to grow with formate as the sole energy source was assessed by replica patching of single puromycin-resistant colonies (propagated with $H_2 + CO_2$) on solid media containing formate (N_2:CO_2 in the gas phase). Those colonies growing much slower than the wild type or not at all with formate were streak purified on formate-free agar plates, exposed to $H_2 + CO_2$, and clonal populations were propagated in liquid media with $H_2 + CO_2$ as substrate. Growth was monitored photometrically at 578 nm (OD_{578}). In vivo labeling of *M. maripaludis* with [^{75}Se]-selenite and analysis of the selenoproteome were conducted as described (Stock et al. 2010).

Molecular methods

Standard methods were used for manipulation of plasmid DNA from *E. coli* (Ausubel et al. 2003). Chromosomal DNA from *M. maripaludis* JJ was isolated via a modified cetyltrimethylammonium bromide method (Murray and Thompson 1980; Metcalf et al. 1996). DNA sequences generated by PCR were determined either by SRD (Bad Homburg, Germany) or by GATC Biotech (Konstanz,

Table 1 Sites of transposon insertion in *M. maripaludis* mutants with impaired formate-dependent growth

Transposon mutant	Nucleotide sequence flanking the mini-MAR367 element (*Tn*)[a]	Gene/locus disrupted[b]
No growth on formate		
V26	…ATGACGATTA-*Tn*-**TA**-TAAACTTA…	MMP1297 (FdhB1)
L39	…ATACCTTGTA-*Tn*-**TA**-TTCTGGGA…	MMP1298 (FdhA1)
B14	…AGTTAGGCTA-*Tn*-**TA**-GTTTATCT…	5′ UTR of MMP1298 (FdhA1)
III38	…GGCTAGTTTA-*Tn*-**TA**-TCTGAACT…	5′ UTR of MMP1298 (FdhA1); 5 bases from B14
W42	…ATCATCCTTA-*Tn*-**TA**-ATTCGAAT…	MMP1300 (hypothetical protein)
W39	…ATATATTATA-*Tn*-**TA**-GTTATCGG…	Upstream of MMP1301 (FdhC)
Slow growth on formate		
K15	…GAGTAAGATA-*Tn*-**TA**-AGATCAGG…	MMP1304 (response regulator)
Prolonged lag during shift from hydrogenotrophic to formate-dependent growth		
BIII13	…CGGAAATGTA-*Tn*-**TA**-AATTTAAA…	MMP1233 (FdhD)
PII49	…TGCTGCAATA-*Tn*-**TA**-ATAAATAT…	MMP1199 (phosphate transport system regulatory protein-related)
Prolonged lag during shift from hydrogenotrophic to formate-dependent growth and slower growth		
RII21	…GCAATAGATA-*Tn*-**TA**-TAACCAGA…	MMP0985 (α subunit of CODH/ACS)
EII2	…GCTGATGTTA-*Tn*-**TA**-TGATATTA…	MMP0980 (γ subunit of CODH/ACS)
GII29	…AACAAGAATA-*Tn*-**TA**-GAATGCCC…	MMP1429 (transcription factor S)

[a] The sequence encoding the transposon is abbreviated as *Tn*, a duplicated TA dinucleotide derived from transposon insertion is given in bold face

[b] According to the genome sequence of *M. maripaludis* S2; deduced proteins are given in parentheses

Germany) employing the BigDye Terminator Cycle Sequencing protocol (Applied Biosystems).

In vitro transposition

A detailed description of the method is published (Rother et al. 2011). In brief, for preparation of recipient DNA for the mini-MAR367 transposition, chromosomal DNA of *M. maripaludis* JJ was partially restricted with *Alu*I and *Dra*I for 15 min with each 0.08 U per µg DNA. Fragments of 1–3 kb were isolated by phenol/chloroform extraction from low melting agarose gel slants (USB, Cleveland, USA), which had been excised from the gels after electrophoretic separation. The transposon delivery plasmid pJJ605 was constructed by removing the *tnp* gene from pJK60 (Zhang et al. 2000), which contains a mini-MAR367 element derived from the insect *mariner* transposon *Himar1* (Lampe et al. 1996), via restriction with *Nde*I and *Bam*HI, treatment with T4 DNA polymerase (Fermentas, St. Leon-Roth, Germany) and religation using T4 DNA ligase (Fermentas). 5 µg recipient DNA, 12.5 µg pJJ605, 12.5 µg bovine serum albumin, and 10–20 nM transposase (see below) were combined in a 50 µl reaction (25 mM 4-(2-hydroxyethyl)-1-piperazineethanesulfonic acid, 100 mM NaCl, 10 mM $MgCl_2$, 2 mM dithiothreitol, pH 7.9) and incubated for 6 h at 25 °C. The reaction was stopped by incubation for 10 min at 75 °C. The DNA was precipitated and transferred into *M. maripaludis* JJ.

Analysis of mini-MAR367 insertion mutants

Randomness and stability of mini-MAR367 insertion in *M. maripaludis* were investigated by DNA hybridization (Southern 1975). To this end, chromosomal DNA was digested with *Bst*YI, electrophoretically separated, transferred to a nylon membrane, and probed with an approximately 500 bp digoxigenin-(DIG-)labeled (Roche, Mannheim, Germany) *Aat*II fragment of pJK301 (Guss et al. 2005) that hybridizes to the *pac* gene within the mini-MAR367 element (Zhang et al. 2000). To identify mini-MAR367 transposon integration sites in *M. maripaludis*, chromosomal DNA from puromycin-resistant mutants was isolated, digested with *Eco*RI, self-ligated using T4 DNA ligase (Fermentas), and subsequently transferred into the pir^+ *E. coli* strain WM1788 (Haldimann and Wanner 2001). There, the circularized DNA containing the transposon was able to replicate, and plasmid-bearing *E. coli* were selected with kanamycin. The plasmid DNA isolated from these transformants was isolated with the High Pure plasmid isolation kit (Roche, Mannheim, Germany) and sequenced using primers IR-5-Rev and IR-3-For (Supplementary Table S1).

Sequencing of genomic regions in M. maripaludis *JJ*

The 10,202 bp genomic region of *M. maripaludis* JJ encoding the genes homologous to MMP1297-MMP1304 of strain S2 (Hendrickson et al. 2004) was amplified by PCR using primers oGR1305-1297/forw and oGR1305-1297/rev (Supplementary Table S1) and cloned into pIJA03 + neo (Lie et al. 2007) via primer-introduced *Mlu*I recognition sites, resulting in pJJGR1305-1297. The region flanked by the *Mlu*I sites was sequenced using primers listed in Supplementary Table S1, and the sequence was deposited at GenBank with the accession number KC342234. To confirm the genomic context of other loci disrupted by mini-MAR367 elements, primers (Supplementary Table S1) derived from the *M. maripaludis* S2 genome sequence were used to amplify by PCR genomic regions from *M. maripaludis* JJ, which were sequenced. These sequences are available on request.

Complementation of mini-MAR367 insertion mutants

Genes disrupted by mini-MAR367 elements, plus ca. 500 bp upstream region (to include potential transcription initiation signals) and ca. 100 bp downstream region (to include potential transcription termination signals), were amplified by PCR (introducing suitable restriction sites) and cloned (via *Spe*I and *Bgl*II) into the *E. coli*/*M. maripaludis* shuttle vector pWLG40NZ-R (Lie and Leigh 2003), which confers neomycin resistance to the latter. Each resulting plasmid was transferred into the corresponding mini-MAR367 mutant, which was then assessed for its formate-dependent growth behavior (see above).

Isolation of RNA

Total RNA was isolated from *M. maripaludis* JJ and from mini-MAR367 insertion mutants grown on $H_2 + CO_2$ or formate. To this end, exponentially growing cultures (OD_{578} 0.4–0.7) were harvested by centrifugation and washed twice with sucrose buffer (800 mM sucrose, 50 mM $NaHCO_3$), followed by RNA isolation using the High Pure RNA isolation Kit (Roche) following the manufacturer's instructions, except omitting the DNase digestion step. Eluted RNA was treated with 1 U RQ1 RNase-free DNase (Promega, Mannheim, Germany) per µg RNA at 37 °C for 90 min and purified using the Nucleospin RNA Clean-up Kit (Macherey–Nagel, Düren, Germany) according to the manufacturer's instructions and stored at −80 °C until use.

Qualitative reverse transcription (RT) PCR

Several overlapping qualitative RT-PCR assays spanning the cluster of MMP1304-MMP1297 homologous open reading frames (ORFs) in *M. maripaludis* JJ were conducted to assess the number and lengths of putative transcripts within this region. For this purpose, 20 µl RT reactions were composed of 100 U SuperScript III reverse transcriptase (Life Technologies, Darmstadt, Germany), 40 U RNase inhibitor (RNaseOUT, Life Technologies, Darmstadt, Germany), 0.5 mM of each dNTP, 1× First Strand RT buffer (50 mM Tris–HCl pH 8.3, 75 mM KCl, 3 mM $MgCl_2$), 5 mM DTT, 0.5 µM gene specific primer, and 1–2 µg RNA. Primers are listed in Supplementary Table S1. RT was carried out at 55 °C for 60 min and was terminated at 70 °C for 15 min. RNA was removed by adding 2 U of *E. coli* RNase H (Life Technologies) and incubation at 37 °C for 20 min. For PCR amplification of cDNA, each 20 µl reaction contained 1 µl of cDNA, 1× Phusion HF buffer, 0.2 mM of each dNTP, 0.4 U Phusion DNA polymerase (Thermo Scientific, St. Leon-Rot, Germany), and 0.5 µM of each primer. Cycling conditions were 98 °C for 30 s, followed by 40 cycles at 98 °C for 10 s, 66 °C for 30 s, and 72 °C for 1 min 30 s. Appropriate controls, containing either template nucleic acid from RT reactions to which no SuperScript III reverse transcriptase had been added, and template nucleic acid that had not been DNase-treated, were included in each RT-PCR assay. PCR products were electrophoretically separated on 1.5 % [wt/vol] agarose gels.

Quantification of fdhA1 *transcripts*

Expression of *fdhA1* gene in *M. maripaludis* JJ and mini-MAR367 insertion mutants was carried out as described previously (Stock et al. 2011) and normalized to the expression of the *mcrB* gene (MMP1555 in the genome of *M. maripaludis* S2) encoding the β subunit of methyl-coenzyme M reductase, which is constitutively expressed in *M. maripaludis* S2 (Xia et al. 2006; Hendrickson et al. 2007). In brief, cDNA from RNA isolated from *M. maripaludis* strains grown on $H_2 + CO_2$ (mini-MAR367 insertion mutants and wild type) or formate (mini-MAR367 insertion mutant K15 and wild type) was generated in 10 µl reactions containing 1× M-MLV reaction buffer (250 mM Tris–HCl, 375 mM KCl, 15 mM $MgCl_2$, 50 mM DTT), 0.5 mM of each dNTP, 80 U M-MLV Reverse Transcriptase RNase H Minus, Point Mutant (Promega), 0.1 µM each primer o1555cDNA and o1298cDNARev (Supplementary Table S1), and 0.5–1 µg RNA at 55 °C for 30 min with a 70 °C step for 15 min to stop the reaction. For quantitative PCR, separate 20 µl reactions for *mcrB* and *fdhA1* containing each 1 µl of cDNA, 1× GoTaq qPCR Mastermix (Promega), and 0.4 µM of each forward and reverse primers were set up (Supplementary Table S1). Initial activation at 95 °C for 2 min was followed by a two-step cycling protocol, comprising denaturation at 95 °C for

15 s and annealing/extension at 60 °C for 60 s over 40 cycles. Negative controls containing template nucleic acid from RT reactions without M-MLV reverse transcriptase were included in each run.

Mapping of transcription start sites

To identify transcription start sites within the *M. maripaludis* JJ genomic region encoding the MMP1304-MMP1297 homologous, ORFs 5′-ends of mRNAs were determined using a modified 5′-RACE protocol (Bose et al. 2009). In a first step to remove rRNA and to enrich for mRNA, DNase treated RNA of the wild type strain was incubated with terminator 5′-phosphate-dependent exonuclease (Epicentre, Madison, USA) at 30 °C for 60 min. Subsequently, a decapped 5′-monophosphorylated RNA terminus was generated using tobacco acid pyrophosphatase (TAP) (Epicentre) according to the manufacturer's instructions and then ligated to the 3′-hydroxyl terminus of an RNA 5′-RACE-adapter (Supplementary Table S1) using T4 RNA Ligase (Fermentas). First strand cDNA was synthesized in separate RT reactions using gene specific reverse primers for each of the genes homologous to MMP1304–MMP1298 (primers 1304rev–1298rev; Supplementary Table S1) and SuperScript III reverse transcriptase according to the manufacturer's instructions, which was followed by a RNase H digestion step as described above. PCR amplifications were carried out as described above, including 0.5 μM 5′RACE adapter primer and 0.5 μM of gene specific primer (primers 5RACE1304rev–5RACE1298rev; Supplementary Table S1). Cycling conditions were 98 °C for 30 s, followed by 40 cycles at 98 °C for 10 s, 67 °C for 30 s, and 72 °C for 1 min. PCR products were separated by electrophoresis, purified using the HiYield PCR clean-up kit (Süd-Laborbedarf, Gauting, Germany), and sequenced. The first base 3′ of the adapter sequence corresponded to the 5′-end of the mRNA in question.

Isolation of Himar1 *transposase*

For overproduction of the hyperactive *Himar1* transposase variant (Lampe et al. 1999), the *tnp* gene was moved from pJK60 via *Nde*I and *Bam*HI to pT7-7 (Tabor and Richardson 1985) resulting in pT7tnp. Plasmid pT7tnp was transferred to *E. coli* BL21 (DE3) (Studier and Moffatt 1986). T7 RNA polymerase-based overexpression of the gene and protein production was induced at an OD_{578} of approximately 1 by addition of 0.5 mM isopropyl-β-D-thiogalactopyranoside and allowed to proceed for 3 h. *Himar1* transposase was purified from inclusion bodies as described (Lampe et al. 1996), except that in buffers benzamidine was omitted, NP-40 was replaced by Nonidet P40, and DEAE-Sepharose was used instead of DEAE-Sephacryl.

Results

Mini-MAR367 insertions in *M. maripaludis* JJ are random and stable

By transforming *M. maripaludis* JJ with in vitro transposition reactions composed of plasmid pJJ605 encoding the mini-*mariner* transposon mini-MAR367, purified hyperactive variant *Himar1* transposase, and genomic restriction fragments, transposon mutants could be isolated by selection on puromycin-containing media at a frequency of 10–30 μg^{-1} recipient DNA. This low frequency probably results from the double homologous recombination which has to occur to place the transposon on the organism's chromosome. When only pJJ605 was used to transform *M. maripaludis*, no puromycin-resistant colonies were obtained (data not shown), which rules out undesired integration of the transposon delivery plasmid into the chromosome. Ten randomly selected puromycin-resistant clones were assessed by Southern hybridization using a probe specific for the *pac* gene contained in the transposon (Fig. 1a). The hybridizing bands were of various sizes indicating that the transposons were randomly inserted at different sites within the genome. Four of these clones were cultivated for 50 generations without selecting for puromycin resistance before the same hybridization experiment was repeated. As seen from Fig. 1b, neither of the hybridizing signals was lost nor changed its size, which strongly suggests that the transposons, once integrated into the chromosome, are stably maintained even in the absence of selection.

Isolation of mini-MAR367 mutants with impaired formate catabolism

After randomness and stability of mini-MAR367 transposition were verified, 2,865 transposon mutants were obtained using $H_2 + CO_2$ as the growth substrates. Through screening of the mutants via replica patching onto formate-containing media, 12 mutants, which were slow growing or not growing under this condition, were phenotypically analyzed in liquid media (Fig. 2). None of the strains grew different than the wild type when $H_2 + CO_2$ served as the growth substrate (data not shown). According to their formate-dependent growth behavior, the mutants could be divided into four categories when compared to the wild type (Fig. 2; Table 1): those not growing on formate at all (strains V26, L39, B14, III38, W42, W39; Table 1 and data not shown), a strain growing more slowly (K15;

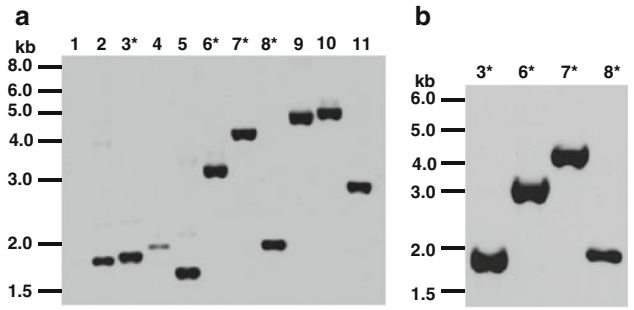

Fig. 1 Randomness and stability of mini-MAR367 transposon insertions in *M. maripaludis*. **a** chromosomal DNA of wild type strain JJ (*lane 1*) and of 10 randomly chosen puromycin-resistant transposon mutants (*lanes 2–11*) was probed with a DIG-labeled *pac*-specific DNA fragment. **b** four of the mutants analyzed in **a** (*asterisks*) were cultivated for 50 generations without selecting for puromycin resistance before the hybridization analysis was repeated; the *lines* on the *left* indicate the migration position of standard fragments of known length in kb

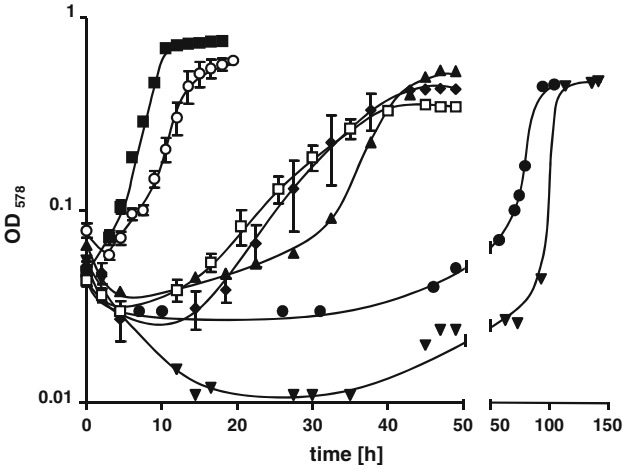

Fig. 2 Formate-dependent growth of *M. maripaludis* transposon mutants. Strains were grown on $H_2 + CO_2$ over night and diluted (4 % [vol/vol]) into formate-containing medium; growth of the wild type strain JJ (*filled squares*) and mini-MAR367 mutants BIII13 (*filled circles*), EII2 (*filled triangles*), GII29 (*open squares*), K15 (*open circles*), PII49 (*filled inverted triangles*), and RII21 (*filled diamonds*) were assessed photometrically; for clarity, the *x*-axis was interrupted at 50 h and subsequently a different scale was applied

Fig. 2), those strains with a prolonged lag phase upon shifting from hydrogenotrophic to formate-dependent growth (strains BIII13 and PII49; Fig. 2), and the strains exhibiting both of the latter two characteristics (RII21, EII2, GII29; Fig. 2). To attribute a genetic defect to the observed phenotype, the transposon integration site was determined in the 12 isolated strains (see "Materials and methods"). Since the genome sequence of *M. maripaludis* JJ is not available, that of strain S2 (Hendrickson et al. 2004) was used for initial comparison with the sequence data obtained. In each case, the sequences flanking a mini-MAR367 could be precisely and unambiguously mapped to a genomic location (Table 1) where the transposon had inserted at a TA dinucleotide, which was duplicated as a result of the mechanism of transposon integration (Lampe et al. 1996). In each case, the genomic context surrounding the mini-MAR367 insertions (at least the up- and downstream gene) was that of the corresponding region in strain S2 (Supplementary Fig. S1). To differentiate ORFs from strain S2 from those of strain JJ, these are, henceforth, expressed in lower case italics with quotation marks.

Identification of genes relevant for formate catabolism

Strain GII29, which grew more slowly on formate and with a prolonged lag phase than the wild type (Fig. 2), carried the transposon in "*mmp1429*", which encodes a homolog of archaeal transcription factor S (Hausner et al. 2000).

Strains RII21 and EII2, which showed a prolonged lag phase and slower growth rate upon the substrate shift (Fig. 2), carried transposons in the genes encoding the α and γ subunits, respectively ("*mmp0985*" and "*mmp0980*"), of the archaeal 5-subunit carbon monoxide dehydrogenase/acetyl-coenzyme A synthase complex (CODH/ACS). When acetate was omitted from the medium, the two strains did not grow with $H_2 + CO_2$ as substrate (Supplementary Fig. S2), which confirms that this enzyme is essential in autotrophic carbon assimilation (Ladapo and Whitman 1990). Further, increasing the concentration of acetate to 50 mM had no effect on the strain's formate-dependent growth phenotype (data not shown).

Strain BIII13, which lagged substantially on formate when compared to the wild type (Fig. 2), carried the mini-MAR367 transposon in "*mmp1233*". Homologous genes are annotated to encode for FdhD, an accessory protein involved in formation of formate dehydrogenase in *E. coli* (Schlindwein et al. 1990). However, the strain started to grow like the wild type after the lag phase, which may indicate that (a) compensatory mutation(s) is (are) required to render this protein dispensable. Strain PII49, which also grew on formate with a substantially prolonged lag phase compared to the wild type (Fig. 2), carried the transposon in "*mmp1199*", encoding a protein similar to PhoU which is involved in regulation of phosphate transport in *E. coli* (Nakata et al. 1984). Neither growth rate nor final cell yield differed noticeably from that of the wild type once the strain started to grow, which is again indicative of (a) compensatory mutation(s) allowing other cellular factors to complement the one disrupted.

Complementing strain BIII13 with a plasmid encoding "*mmp1233*" (*fdhD*) including ca. 500 bp of its upstream and ca. 100 bp of its downstream region fully restored the strain's ability to grow with formate such as the wild type (Supplementary Fig. S3), which strongly indicates that the

mutant phenotype was solely caused by lack of *fdhD*. Applying the same complementation strategy to GII29, i.e., transferring a plasmid encoding "*mmp1429*" including ca. 500 bp of its upstream and ca. 100 bp of its downstream region, partly restored the strain's phenotype. While its growth rate and final optical density approached that of the wild type, it still displayed a substantial lag phase before formate-dependent growth started (Supplementary Fig. S3). Thus, the phenotype of GII29 is caused not only by lack of "*mmp1429*", but probably also by a polar effect which changed expression of (a) vicinal gene(s) as well.

A multi-gene locus in *M. maripaludis* JJ important for formate catabolism

According to the genome sequence of *M. maripaludis* S2, the seven remaining mutants had the mini-MAR367 element inserted into one ca. 10 kb genomic region also encoding Fdh1. To verify that gene organization of the *M. maripaludis* strains S2 and JJ was similar and, thus, that the transposon insertions in strains K15, W39, W42, III38, B14, L39, and V26 (Table 1) were indeed located in the same genomic region, it was amplified by PCR using chromosomal DNA of *M. maripaludis* JJ as template, cloned, and sequenced (see "Materials and methods"). The 10,202 bp sequence of *M. maripaludis* JJ (Fig. 3a) was very similar to the corresponding region from *M. maripaludis* S2, with overall nucleotide sequence identity of 97 %. On the level of deduced amino acid sequences of the ORFs, identities between the two *M. maripaludis* strains ranged from 97 % (MMP1303) to 100 % (MMP1298), Supplementary Table S2.

The gene ("*mmp1304*") interrupted in strain K15, which grew more slowly on formate than the wild type (Fig. 2), encodes a putative transcriptional regulator. Directly downstream of this gene, a putative sensor histidine kinase is encoded indicating that the two resulting proteins may constitute a two component regulatory system involved in formate metabolism (Fig. 3). Interestingly, all six remaining mutants (V26, L39, B14, III38, W42, W39) that carried the transposon in the vicinity of "*mmp1304*" were unable to grow with formate as the sole source of energy. In strain W39, the mini-MAR367 element was located in the intergenic region between the "*mmp1302*" and "*mmp1301*", of which the latter encodes a putative formate transporter (FdhC). Strain W42 carried the transposon within "*mmp1300*" encoding a hypothetical protein found in all *Methanococcus* species with known genome sequences. Strains B14 and III38 carried a transposon at positions only five nucleotides apart from each other, in the putative 5′-untranslated region (5′-UTR) of the *fdhA1* gene ("*mmp1298*"), which encodes the large subunit of one of two isoforms of Fdh in *M. maripaludis*, FdhA1 (Wood et al. 2003). While in strain L39, the coding region of *fdhA1* was disrupted; strain V26 carried mini-MAR367 in "*mmp1297*", which encodes the small subunit of Fdh1, FdhB1. Beside the genes disrupted by mini-MAR367 elements, this region also encodes a putative carbonic

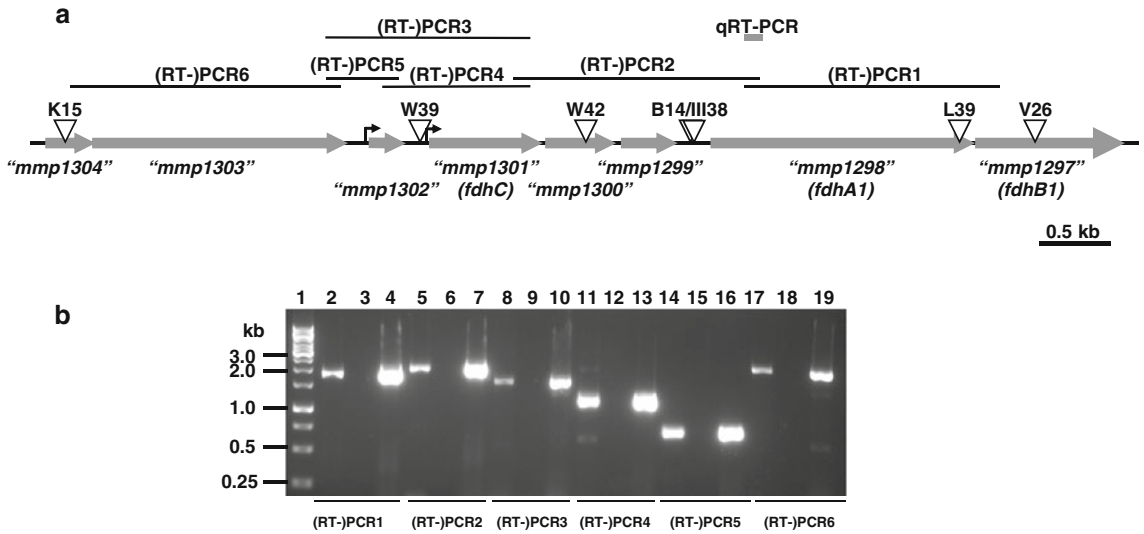

Fig. 3 Analysis of the genomic region in *M. maripaludis* JJ encoding Fdh1. **a** schematic overview of the gene organization (*gray arrows* with gene names), transposon insertion sites (*open triangles* with strain designation), transcription start sites determined (*right angled arrows*), mRNA verified (*black lines* with RT-PCR reaction assay number as depicted in **b**), and the part of *fdhA1* used for transcript quantification (qRT-PCR, *gray line*). **b** verification of overlapping transcripts by qualitative RT-PCR using oligonucleotides listed in Supplementary Table S1; *lane 1*, DNA standard (with fragment sizes given in kb on the *left*); *lanes 2, 5, 8, 11, 14, 17*, PCR amplification of cDNA; *lanes 3, 6, 9, 12, 15, 18*, reactions without reverse transcriptase; *lanes 4, 7, 10, 13, 16, 19*, reactions without DNase treatment; assays (RT-PCRs) are numbered according to the overview depicted in **a**

anhydrase ("*mmp1299*") and a small protein ("*mmp1302*") shown to bind selenium in *Methanococcus vannielii* (Self et al. 2004).

Mapping of the Fdh1 encoding transcripts

Like in *M. maripaludis* strain S2, the homologous genes in *M. maripaludis* JJ have the same orientation with intergenic regions ranging from 27 bp (upstream of "*mmp1303*") to 300 bp (upstream of "*mmp1298*", Fig. 3a), which could indicate that "*mmp1304*" to "*mmp1297*" constitutes an operon and are monocistronically transcribed. To address this issue, qualitative RT-PCR analyses of the regions potentially bridging the coding regions within the putative transcript were conducted in the wild type strain (Fig. 3b). For every junction of two genes within this region of the genome, mRNA could clearly be detected, which demonstrates that *M. maripaludis* JJ contains transcripts encoding "*mmp1304*" through "*mmp1297*" (see Fig. 3a, top). To identify mRNA 5′-termini, i.e., transcription start sites within this genomic region, 5′-RACE was conducted (see "Materials and methods"), which identified two transcription start sites: one upstream of "*mmp1302*" and one upstream of "*mmp1301*" (Fig. 3a and Supplementary Fig. S4). Although we could clearly detect mRNA encoding "*mmp1304*" and "*mmp1303*" (Fig. 3b, lane 17) and mRNA encoding "*mmp1303*", "*mmp1302*", and "*mmp1301*" (Fig. 3b, lane 8) which strongly suggested transcription initiation upstream of "*mmp1304*", we failed to detect an mRNA 5′-end in this region (despite numerous attempts using different reverse transcriptases and several different conditions for adapter ligation, cDNA synthesis, and PCR). If the 5′-region of the mRNA formed stable secondary structures adapter ligation or TAP treatment could be diminished. Also, strain K15, which carries the transposon in the first gene of this putative operon, was not severely affected in its formate-dependent growth, which could mean that transcription of the operon starting from the putative "*mmp1304*" promoter is of minor physiological relevance. No transcription start site in the 5′-vicinity of "*mmp1298*" (*fdhA1*) could be found, and "*mmp1298*" (*fdhA1*) and "*mmp1297*" (*fdhB1*) appear to be cotranscribed due to mRNA detected encoding both genes and only 35 bp intergenic region between the two genes. Taken together, these findings strongly suggest that *M. maripaludis* JJ contains three different *fdh1*-encoding transcript species of various lengths.

Expression of *fdhA1* in mini-MAR367 mutants

The genomic region comprising "*mmp1304*" through "*mmp1297*" encodes, beside Fdh1, other functions potentially involved in formate metabolism. Thus, the formate-dependent growth impairment observed in the transposon mutants could either be due to the absence of the product of the respective disrupted gene, or to impaired *fdh1* expression caused by polar effects inflicted by the transposons. In order to address the latter possibility, *fdhA1* transcript abundance was determined in the mini-MAR367 mutants K15, W39, W42, B14, and V26 (Table 1) by quantitative RT-PCR (see "Materials and methods"). Compared to the wild type, *fdhA1* abundance in W39, W42, and B14 was at least 20-fold reduced (Table 2), which strongly argues in favor of polar effects caused by the transposons. Abundance of *fdhA1*-mRNA in V26 was also somewhat reduced compared to the wild type, even if only by 20 %. Since in strain V26 the last gene in the Fdh1-encoding operon was disrupted, which should have no effect on transcription initiation, this observation would be consistent with a reduced half-life of the transcript. Surprisingly, *fdhA1* transcript abundance was higher in strain K15 than in the wild type regardless if grown on $H_2 + CO_2$ or formate (Table 2).

Selenium incorporation in mini-MAR367 mutants

Since Fdh in *M. maripaludis* JJ contains selenocysteine, its presence in the mini-MAR367 mutants K15, W39, W42, B14, and V26 was assessed by in vivo labeling with [^{75}Se] and electrophoretic separation of the crude extracts by dodecyl sulfate polyacrylamide gel electrophoresis (Fig. 4). While the ability to synthesize selenoproteins was unaffected in the mutants, only V26 contained a labeled macromolecule at the position in the gel where Fdh migrates in the wild type (Fig. 4, lane 1), albeit at a much lower level (Fig. 4, lane 4), which suggests rapid turnover of FdhA1 in the absence of FdhB1. In strains B14, W39, and W42 (Fig. 4, lanes 2, 5, and 6, respectively), the absence of sec-containing FdhA is consistent with the *fdhA1* mRNA abundances determined, which explains why

Table 2 Relative abundance of *fdhA1* transcript in *M. maripaludis*

	Growth substrate	
Strain	$H_2 + CO_2$	Formate
JJ (wild type)	34.0 ± 11.8	61 ± 36
K15	208.0 ± 88.7	138.6 ± 53.6
W39	1.6 ± 0.2	ND
W42	0.6 ± 0.4	ND
B14	1.0 ± 0.3	ND
V26	28.7 ± 12.1	ND

Numbers given are in arbitrary units and were obtained by normalization against abundance of *mcrB* (encoding a subunit of methyl-coenzyme M reductase) which was set to 100. Values are averages from triplicate results obtained with at least two independent cultures, ± indicates the standard deviation

ND not determined

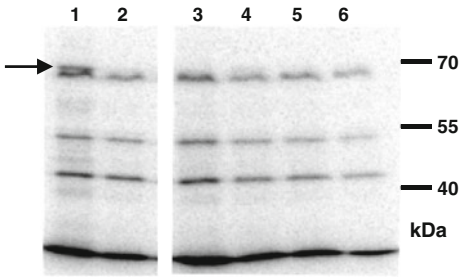

Fig. 4 Selenoprotein synthesis in *M. maripaludis*. Autoradiograph of a 10 % sodium dodecyl sulfate polyacrylamide gel (Laemmli 1970) after electrophoresis of ^{75}Se-labeled cell lysates; *lane 1*, wild type strain JJ; *lane 2*, B14; *lane 3*, K15; *lane 4*, V26; *lane 5*, W39; *lane 6*, W42; the *arrow* depicts the migration position of selenocysteine-containing FdhA; migration positions of standard proteins (in kDa) are indicated on the *right*

these strains could not grow with formate as the sole energy source.

Discussion

The aim of the present study was to demonstrate the feasibility of a genetic strategy to identify factors involved in formate-dependent growth of *M. maripaludis* JJ. The tool employed was an engineered insect transposon, which, like all transposons, can create polar effects on expression of genes adjacent to the one disrupted. This possibility has to be taken into account when correlating the phenotype with the transposon location. Also, compensatory mutations can occur under high selection pressure, like, for example, the conditions employed here, i.e., the ability to grow on formate. 2,865 transposon mutants were created, and assuming a similar genome size for *M. maripaludis* strain JJ as that of strain S2 (approximately 1.8 Mbp) and an average gene size of 0.9 kb, the number of random transposon mutants should suffice to disrupt every nonessential gene at least once. However, since most of the factors were identified (by tagging with a transposon) only once as being relevant for formate utilization, the number of mutants screened might still be too low to fully saturate the genome.

A factor unambiguously correlated to formate catabolism of *M. maripaludis* JJ by complementation was FdhD (strain BIII13, encoded by "*mmp1233*"). Although the exact reaction FdhD catalyzes is unknown, it was shown to be required for maturation of Fdh of *E. coli* (Schlindwein et al. 1990). Still, the factor appears not to be absolutely required in *M. maripaludis* for formate utilization indicating that a FdhD-independent path exists to generate active Fdh.

Previously unrecognized as being involved in formate-dependent growth is "*mmp1429*", encoding a homolog of archaeal transcription factor S (Hausner et al. 2000). When provided in *trans*, the gene partly reverted the formate-dependent growth defect of the respective mini-MAR367 mutant GII29 (Supplementary Fig. S3). The protein was shown to aid fidelity of transcription via its RNA cleavage activity (Lange and Hausner 2004). The shift from $H_2 + CO_2$ to formate as the sole energy source probably requires formate-specific genes to be expressed at a high rate, which could be negatively affected in the absence of transcription factor S, leading to the growth phenotype observed. Alternatively, it is feasible that in *M. maripaludis* factors involved in formate-dependent, but not H_2-dependent, energy metabolism interact with the transcription apparatus thereby allowing rapid response to changing substrate conditions. In vitro evidence suggests that in *Methanocaldococcus jannaschii* H_2-dependent N_5,N_{10}-methenyltetrahydromethanopterin dehydrogenase interacts with a prolyl-specific $tRNA^{Pro}$, thereby connecting energy metabolism and mRNA translation (Oza et al. 2012).

Since all other genes tagged with a transposon and apparently affecting formate-dependent growth of *M. maripaludis* JJ were located in presumed larger transcriptional units, complementation of the respective mini-MAR367 mutants with the genes disrupted was not attempted as polar effects could have influenced the phenotype screened for. Still, the information gained by correlating the formate-dependent phenotype with the location of the transposon on the chromosome is valuable, it could indicate that the vicinally encoded genes share a common functionality. One such example was "*mmp1199*" (disrupted in strain PII49) which encodes a protein similar to a regulatory protein involved in phosphate transport [PhoU (Nakata et al. 1984)]. However, it appears unlikely that "*mmp1199*" is involved in phosphate metabolism in *M. maripaludis* JJ because the gene is located in a potential operon also encoding a putative nitrate/sulfonate/bicarbonate ABC transporter (Supplementary Fig. S1), suggesting that "*mmp1199*" is involved in regulation of this transporter. The substrate translocated is unknown, but it is tempting to speculate that it is relevant for formate-dependent growth, such as formate or selenium. Intracellular depletion of either would prevent the mutant from shifting from $H_2 + CO_2$ to formate, the former due to lack of growth substrate, the latter because formate dehydrogenase in *M. maripaludis* is selenium-dependent (Rother et al. 2003). Whether loosing "*mmp1199*" directly or indirectly affected formate-dependent growth, its function can obviously be fully compensated by other factors in the cell.

As two independently isolated strains (RII21 and EII2) in which subunits of CODH/ACS were disrupted by mini-MAR367 elements exhibited similar growth defects on formate, this enzyme appears to play a more important role

during growth on formate than on $H_2 + CO_2$. However, the basis for this difference in importance is not apparent because the pathway for CO_2 fixation is the same under both growth conditions, the only difference is the electron donor (reduced F_{420} for formate-dependent and H_2 for hydrogenotrophic growth). Reduced ferredoxin, required for both catabolism and anabolism, can be generated from either of the electron donors, (Costa et al. 2010; Lie et al. 2012). Therefore, the lack of CODH/ACS may exert an indirect effect. Because exogenous acetate has to be taken up and activated to acetyl-CoA to enter anabolism in the absence of CODH/ACS, the observed phenotype may indicate that during formate-dependent growth, acetate is not as efficiently taken up than during hydrogenotrophic growth. As formate and acetate would have to be actively transported into the cell at the pH of the medium used, competition for a common transport system could be a plausible explanation for the phenotype observed.

Of the 12 mini-MAR367 mutants characterized here, seven carried the transposon in a 10.2 kb genomic region encoding Fdh1. The fact that disrupting the structural genes for Fdh1 (strains L39 and V26) in *M. maripaludis* JJ leads to the inability to grow with formate supports the previous proposal that Fdh2 does not suffice to support formate-dependent growth (Stock et al. 2011). The inability of four of the mutants (B14, III38, W42, W39) to grow on formate can be explained with the strongly decreased abundance of *fdhA1* mRNA due to polar effects of the transposons inserted. Indeed, our analyses showed that either "*mmp1301*"–"*mmp1297* or "*mmp1302*"–"*mmp1297*" are expressed from alternative promoters upstream of "*mmp1301"* and "*mmp1302*", respectively. This notion is consistent with observations made in *M. maripaludis* S2; fusing a reporter gene to a 192-bp region upstream of MMP1301 (*fdhC*) resulted in lower amplitude of formate-dependent transcriptional regulation than when the same region, extended 5′ by MMP1302 and including its upstream region, was used (Wood et al. 2003). The fact that four genes ("*mmp1302*"–"*mmp1299*") are coexpressed with the essential *fdh1* also strongly argues for a common functionality, i.e., their relevance for utilization of formate. For example, beside the structural subunits of Fdh1 ("*mmp1297*" and "*mmp1298*"), the protein encoded by "*mmp1302*" in this region is thought to serve a transport and storage function for selenium (Stadtman 2004), which is a constituent of Fdh in *M. maripaludis* in the form of sec. Since no selenium-independent Fdh is present in *M. maripaludis* providing an intracellular pool of selenium for sec, synthesis would be beneficial for the organism growing on formate.

Gene "*mmp1304*" (disrupted in strain K15) encodes a putative transcriptional regulator, and its loss leads to increased *fdhA1* abundance regardless whether $H_2 + CO_2$ or formate serves as growth substrate. Therefore, impairment of derepression of "*mmp1302*"–"*mmp1297*" transcription seems a plausible explanation for the observed phenomenon. However, why *fdhA1* abundance was even higher in K15 than in the formate-grown wild type (which presumably corresponds to the highest physiologically meaningful level of expression) cannot be explained with the present data. Presumably, additional secondary effects lead to overexpression of the gene. The absence of sec-containing FdhA1 in strain K15 also can not be explained easily as the level of encoding mRNA was even higher than in the wild type (compare Table 2 and Fig. 4, lane 3). This strain still grows with formate, albeit more slowly than the wild type (Fig. 2), which indicates that it probably synthesizes Fdh but without incorporating sec. Evidence for a selenium-independent route effecting cysteine insertion at UGA codons in selenoprotein mRNAs, which utilizes the enzymes for sec synthesis, and incorporation in eukaryotes has been presented (Xu et al. 2011). For *Methanococcus*, a different mechanism for cysteine insertion at UGA codons in selenoprotein mRNAs employing the cysteinyl-$tRNA^{cys}$ biosynthetic route has also been proposed (Yuan et al. 2010). Still, how sec-independent Fdh may be synthesized when the factor encoded by "*mmp1304*" is absent—while synthesis of the other selenoproteins remains unaffected—is difficult to conceive and awaits detailed experimental analysis.

It is noteworthy that in *M. maripaludis* JJ five *trans*-active factors involved in sec synthesis and incorporation are known which, when deleted, result in the inability of the organism to grow with formate (Rother et al. 2003; Stock et al. 2010, 2011). Still, none of those were found in the present study, possibly due to an insufficient number of transposon mutants screened. On the other hand, it is much more likely for each transposition event to insert a transposon into the 10.2 kb genome region encoding "*mmp1304*"–"*mmp1297*", than to "hit" an average length gene, which would impose a statistical bias against isolation of truly "random" mutants based on formate-dependent growth phenotype. Alternatively, not finding factors for sec synthesis and incorporation could also be due to the polyploidy of *M. maripaludis* (Hildenbrand et al. 2011). If not all copies of a gene encoding such a factor are inactivated and even only a few wild type alleles remain in the cell, they would be able to synthesize sec-containing Fdh and, thus, to grow on formate, as was shown for *selD* (encoding selenophosphate synthetase) in *M. maripaludis* S2 (Hildenbrand et al. 2011).

In conclusion, we have identified via random mutagenesis several factors directly or indirectly affecting formate-dependent catabolism of *M. maripaludis* JJ. Among them were genes previously not recognized to play such a role, and genes cotranscribed with the structural genes, encoding

the main formate dehydrogenase of the organism, which are, thus, most likely intimately connected to the formate-dependent physiology of the organism. By correlating disruption of genes to detrimental effects for the organism's formate-dependent physiology, we could narrow down their potential physiological function, thus aiding their analysis in the future.

Acknowledgments We thank Deniz Seyhan (Frankfurt am Main, Germany) for his help in screening mini-MAR367 mutants and Marina Totrova for excellent technical assistance. The authors declare that they have no conflict of interest. This work was supported by a grant from the Deutsche Forschungsgemeinschaft (via SFB 902) to M.R.

References

Ausubel FM, Brent R, Kingston RE et al (2003) Current protocols in molecular biology. J. Wiley & Sons, Inc., New York

Bose A, Kulkarni G, Metcalf WW (2009) Regulation of putative methyl-sulphide methyltransferases in *Methanosarcina acetivorans* C2A. Mol Microbiol 74:227–238

Costa KC, Wong PM, Wang T et al (2010) Protein complexing in a methanogen suggests electron bifurcation and electron delivery from formate to heterodisulfide reductase. Proc Natl Acad Sci USA 107:11050–11055

Costa KC, Yoon SH, Pan M, Burn JA, Baliga NS, Leigh JA (2013) Effects of H_2 and formate on growth yield and regulation of methanogenesis in *Methanococcus maripaludis*. J Bacteriol 195:1456–1462

Deppenmeier U, Müller V (2008) Life close to the thermodynamic limit: how methanogenic archaea conserve energy. In: Schäfer G, Penefsky HS (eds) Bioenergetics: energy conservation and conversion. Springer, Heidelberg, pp 123–152

Ferry JG (1990) Formate dehydrogenase. FEMS Microbiol Rev 87:377–382

Fiedler S, Wirth R (1988) Transformation of bacteria with plasmid DNA by electroporation. Anal Biochem 170:38–44

Guss AM, Mukhopadhyay B, Zhang JK, Metcalf WW (2005) Genetic analysis of *mch* mutants in two *Methanosarcina* species demonstrates multiple roles for the methanopterin-dependent C-1 oxidation/reduction pathway and differences in H_2 metabolism between closely related species. Mol Microbiol 55:1671–1680

Haldimann A, Wanner BL (2001) Conditional-replication, integration, excision, and retrieval plasmid-host systems for gene structure-function studies of bacteria. J Bacteriol 183:6384–6393

Hausner W, Lange U, Musfeldt M (2000) Transcription factor S, a cleavage induction factor of the archaeal RNA polymerase. J Biol Chem 275:12393–12399

Hendrickson EL, Kaul R, Zhou Y et al (2004) Complete genome sequence of the genetically tractable hydrogenotrophic methanogen *Methanococcus maripaludis*. J Bacteriol 186:6956–6969

Hendrickson EL, Haydock AK, Moore BC, Whitman WB, Leigh JA (2007) Functionally distinct genes regulated by hydrogen limitation and growth rate in methanogenic Archaea. Proc Natl Acad Sci USA 104:8930–8934

Hildenbrand C, Stock T, Lange C, Rother M, Soppa J (2011) Genome copy numbers and gene conversion in methanogenic archaea. J Bacteriol 193:734–743

Jones WJ, Paynter MJB, Gupta R (1983) Characterization of *Methanococcus maripaludis* sp. nov., a new methanogen isolated from salt marsh sediment. Arch Microbiol 135:91–97

Ladapo J, Whitman WB (1990) Method for isolation of auxotrophs in the methanogenic archaebacteria: role of the acetyl-CoA pathway of autotrophic CO_2 fixation in *Methanococcus maripaludis*. Proc Natl Acad Sci USA 87:5598–5602

Laemmli UK (1970) Cleavage of structural proteins during the assembly of the head of bacteriophage T4. Nature 227:680–685

Lampe DJ, Churchill ME, Robertson HM (1996) A purified *mariner* transposase is sufficient to mediate transposition in vitro. EMBO J 15:5470–5479

Lampe DJ, Akerley BJ, Rubin EJ, Mekalanos JJ, Robertson HM (1999) Hyperactive transposase mutants of the *Himar1 mariner* transposon. Proc Natl Acad Sci USA 96:11428–11433

Lange U, Hausner W (2004) Transcriptional fidelity and proofreading in Archaea and implications for the mechanism of TFS-induced RNA cleavage. Mol Microbiol 52:1133–1143

Leigh JA, Albers SV, Atomi H, Allers T (2011) Model organisms for genetics in the domain Archaea: methanogens, halophiles, *Thermococcales* and *Sulfolobales*. FEMS Microbiol Rev 35:577–608

Lie TJ, Leigh JA (2003) A novel repressor of *nif* and *glnA* expression in the methanogenic archaeon *Methanococcus maripaludis*. Mol Microbiol 47:235–246

Lie TJ, Dodsworth JA, Nickle DC, Leigh JA (2007) Diverse homologues of the archaeal repressor NrpR function similarly in nitrogen regulation. FEMS Microbiol Lett 271:281–288

Lie TJ, Costa KC, Lupa B, Korpole S, Whitman WB, Leigh JA (2012) Essential anaplerotic role for the energy-converting hydrogenase Eha in hydrogenotrophic methanogenesis. Proc Natl Acad Sci USA 109:15473–15478

Lupa B, Hendrickson EL, Leigh JA, Whitman WB (2008) Formate-dependent H_2 production by the mesophilic methanogen *Methanococcus maripaludis*. Appl Environ Microbiol 74:6584–6590

Metcalf WW, Zhang JK, Shi X, Wolfe RS (1996) Molecular, genetic, and biochemical characterization of the *serC* gene of *Methanosarcina barkeri* Fusaro. J Bacteriol 178:5797–5802

Murray MG, Thompson WF (1980) Rapid isolation of high molecular weight plant DNA. Nucleic Acids Res 8:4321–4325

Nakata A, Amemura M, Shinagawa H (1984) Regulation of the phosphate regulon in *Escherichia coli* K-12: regulation of the negative regulatory gene phoU and identification of the gene product. J Bacteriol 159:979–985

Oza JP, Sowers KR, Perona JJ (2012) Linking energy production and protein synthesis in hydrogenotrophic methanogens. Biochemistry 51:2378–2389

Rother M, Mathes I, Lottspeich F, Böck A (2003) Inactivation of the *selB* gene in *Methanococcus maripaludis*: effect on synthesis of selenoproteins and their sulfur-containing homologs. J Bacteriol 185:107–114

Rother M, Sattler C, Stock T (2011) Studying gene regulation in methanogenic archaea. Methods Enzymol 494:91–110

Sarmiento BF, Leigh JA, Whitman WB (2011) Genetic systems for hydrogenotrophic methanogens. Methods Enzymol 494:43–73

Schlindwein C, Giordano G, Santini CL, Mandrand MA (1990) Identification and expression of the *Escherichia coli fdhD* and *fdhE* genes, which are involved in the formation of respiratory formate dehydrogenase. J Bacteriol 172:6112–6121

Self WT, Pierce R, Stadtman TC (2004) Cloning and heterologous expression of a *Methanococcus vannielii* gene encoding a selenium-binding protein. IUBMB Life 56:501–507

Southern EM (1975) Detection of specific sequences among DNA fragments separated by gel electrophoresis. J Mol Biol 98:503–517

Stadtman T (2004) *Methanococcus vannielii* selenium metabolism: purification and N-terminal amino acid sequences of a novel selenium-binding protein and selenocysteine lyase. IUBMB Life 56:427–431

Stock T, Rother M (2009) Selenoproteins in archaea and gram-positive bacteria. Biochim Biophys Acta 1790:1520–1532

Stock T, Selzer M, Rother M (2010) *In vivo* requirement of selenophosphate for selenoprotein synthesis in archaea. Mol Microbiol 75:149–160

Stock T, Selzer M, Connery S, Seyhan D, Resch A, Rother M (2011) Disruption and complementation of the selenocysteine biosynthesis pathway reveals a hierarchy of selenoprotein gene expression in the archaeon *Methanococcus maripaludis*. Mol Microbiol 82:734–747

Studier FW, Moffatt BA (1986) Use of bacteriophage T7 RNA polymerase to direct selective high-level expression of cloned genes. J Mol Biol 189:113–130

Tabor S, Richardson CC (1985) A bacteriophage T7 RNA polymerase/promoter system for controlled exclusive expression of specific genes. Proc Natl Acad Sci USA 82:1074–1078

Thauer RK (1998) Biochemistry of methanogenesis: a tribute to Marjory Stephenson. Microbiology 144:2377–2406

Tumbula DL, Makula RA, Whitman WB (1994) Transformation of *Methanococcus maripaludi*s and identification of a *Pst*I-like restriction system. FEMS Microbiol Lett 121:309–314

Wanner BL (1986) Novel regulatory mutants of the phosphate regulon in *Escherichia coli* K-12. J Mol Biol 191:39–58

Whitman WB, Shieh J, Sohn S, Caras DS, Premachandran U (1986) Isolation and characterisation of 22 mesophilic methanococci. Syst Appl Microbiol 7:235–240

Wood GE, Haydock AK, Leigh JA (2003) Function and regulation of the formate dehydrogenase genes of the methanogenic archaeon *Methanococcus maripaludis*. J Bacteriol 185:2548–2554

Xia Q, Hendrickson EL, Zhang Y et al (2006) Quantitative proteomics of the archaeon *Methanococcus maripaludis* validated by microarray analysis and real time PCR. Mol Cell Proteomics 5:868–881

Xu XM, Turanov AA, Carlson BA et al (2011) Targeted insertion of cysteine by decoding UGA codons with mammalian selenocysteine machinery. Proc Natl Acad Sci USA 107:21430–21434

Yuan J, Hohn MJ, Sherrer RL, Palioura S, Su D, Söll D (2010) A tRNA-dependent cysteine biosynthesis enzyme recognizes the selenocysteine-specific tRNA in *Escherichia coli*. FEBS Lett 584:2857–2861

Zhang JK, Pritchett MA, Lampe DJ, Robertson HM, Metcalf WW (2000) *In vivo* transposon mutagenesis of the methanogenic archaeon *Methanosarcina acetivorans* C2A using a modified version of the insect *mariner*-family transposable element *Himar1*. Proc Natl Acad Sci USA 97:9665–9670